^{127}I NQR and Crystal Structure Studies of $[N(CH_3)_4]_2CdI_4$

Hideta Ishihara, Keizo Horiuchi[a], Thorsten M. Gesing[b], Shi-qi Dou[b], J.-Christian Buhl[b], and Hiromitsu Terao[c]

Faculty of Culture and Education, Saga University, Saga 840-8502, Japan
[a] Faculty of Science, University of the Ryukyus, 1 Senbaru, Okinawa 903-0213, Japan
[b] Institut für Mineralogie, Universität Hannover, Welfengarten 1, D-30167 Hannover
[c] Faculty of Integrated Arts and Sciences, Tokushima University, Tokushima 770-8502, Japan

Reprint requests to Prof. H. I.; E-mail: isiharah@cc.saga-u.ac.jp

Z. Naturforsch. **55 a,** 225–229 (2000); received October 13, 1999

Presented at the XVth International Symposium on Nuclear Quadrupole Interactions, Leipzig, Germany, July 25 - 30, 1999.

The temperature dependence of ^{127}I NQR and DSC as well as the crystal structure at room temperature of the title compound were determined. This compound shows a first-order phase transition of an order-disorder type at 245 K. Eight ^{127}I(ν_1: $m = \pm\frac{1}{2} \leftrightarrow \pm\frac{3}{2}$) NQR lines of 79.57, 81.86, 82.56, 83.36, 84.68, 87.72, 88.34, and 88.86 MHz, and corresponding eight ^{127}I(ν_2: $m = \pm\frac{3}{2} \leftrightarrow \pm\frac{5}{2}$) NQR lines were observed at liquid nitrogen temperature. Three ^{127}I(ν_1) NQR lines with an intensity ratio of 1:1:2 in the order of decreasing frequency were observed just above the transition point and two NQR lines except for the middle-frequency line disappeared around room temperature. This temperature behavior of NQR lines is very similar to that observed in $[N(CH_3)_4]_2HgI_4$. Another first-order phase transition takes place at 527 K. The structure of the room-temperature phase was redetermined: orthorhombic, Pnma, $Z = 4$, $a = 1342.8(3)$, $b = 975.7(2)$, $c = 1696.5(3)$ pm. The NQR result of three lines with an intensity ratio of 1:1:2 is in agreement with this structure. The thermal displacement parameters of atoms in both cations and anions are large.

Key words: NQR; DSC; Crystal Structure; Phase Transition.

Introduction

Kallel et al. reported that $[N(CH_3)_4]_2CdI_4$ crystallizes at room temperature in orthorhombic β-K_2SO_4 structure type with space group Pnma [1]. Many compounds belonging to the A_2BX_4 family with β-K_2SO_4 structure undergo successive phase transitions. From DTA studies Sato et al. reported that $[N(CH_3)_4]_2CdI_4$ shows phase transitions around 244 K [2]. The crystal structure of the room temperature phases of $[N(CH_3)_4]_2MX_4$ (M = Zn, Cd, Hg; X = Cl, Br, I) is orthorhombic β-K_2SO_4 structure [1 - 8]. Among the nine compounds, $[N(CH_3)_4]_2ZnCl_4$ has been most extensively studied because it undergoes successive phase transitions and has an incommensurate and ferroelectric phase. Furthermore $[N(CH_3)_4]_2ZnBr_4$ and $[N(CH_3)_4]_2CdBr_4$ as well as $[N(CH_3)_4]_2MnBr_4$ and $[N(CH_3)_4]_2CoBr_4$ are well known to show anomalous ferroelasticity. However, the title compound has been little studied so far. We measured the temperature dependence of ^{127}I NQR and DSC, and redetermined the crystal structure.

Experimental

0.2 mol of $[N(CH_3)_4]I$ and 0.1 mol of $CdCO_3$ were mixed in a hydroiodic acid solution containing 0.4 mol of HI. The precipitate, appearing immediately, could be completely dissolved by adding about 4 l water. The pH value of the solution was kept below 3 by adding an excess of hydroiodic acid. By evaporating the solvent, white needles appeared. NQR was observed by using superregenerative type spectrometers. DSC measurements were carried out above 130 K with a differential scanning calorimeter DSC220 from Seiko Instruments Inc. under the following conditions: sample weight ca. 10 mg, heating rate 2 - 10 K min^{-1} with flowing dry N_2 gas at

0932–0784 / 00 / 0100–0225 $ 06.00

Table 1. Experimental conditions for the crystal structure determination and crystallographic data of *bis*(tetramethylammonium) tetraiodocadmate(II), $[N(CH_3)_4]_2CdI_4$. Diffractometer: Stoe IPDS; wavelength: 71.07 pm (MoKα); Monochromator: Graphite(002); Scan: $2\theta/\omega = 1/1$. $C_8H_{24}N_2CdI_4$: MW = 768.32.

Crystal Size/mm^3	0.2×0.1×0.25
Temperature / K	293(2)
Absorption Coeff. / mm^{-1}	6.523
2θ-range for data collected	$3.86 \leq 2\theta/° \leq 48.34$
Index Ranges	$-15 \leq h \leq 15$, $-11 \leq k \leq 11$, $-19 \leq k \leq 19$
Space Group	Pnma
Cell Dimensions: *a*/pm	1342.8(3)
b/pm	975.7(2)
c/pm	1696.5(3)
$V \times 10^{-6}$/pm^3	2222.7(8)
Z (formula units/cell)	4
ρ_{calc}/(Mg·m^{-3})	2.296
$F(000)$	1384
Refls Collected/Measured	12411/1889
R_{int}	0.1652
Obs. Refls ($I > 2\sigma(I_0)$)	466
Restraints/Parameters	2/161
R (observed data)	$R(F) = 0.0278$: $wR(F^2) = 0.0359$
R (all data)	$R(F) = 0.1721$: $wR(F^2) = 0.0452$
Goodness-of-fit (observed/all data)	$S(F^2) = 0.854/0.486$
Largest e-Density Peak and Hole $\times 10^6$/(e·pm^{-3})	0.332 and –0.367
Extinction Corr. Coeff.	0.00037(3)
Point Positions	Cd(1), I(1), I(2), N(1), C(11), C(12), N(2), C(21), C(22) in 4c, I(4), C(13), C(23) in 8d

Table 2. Atomic coordinates and equivalent isotropic displacement parameters U_{eq} (10^{-1} pm^2). U_{eq} is defined as 1/3 of the trace of the U_{ij} tensor: the temperature factor T has the from $T = \exp\{-2\pi^2(U_{11}h^2a^{*2} + U_{22}k^2b^{*2} + U_{33}l^2c^{*2} + 2U_{12}hka^*b^* + 2U_{13}hla^*c^* + 2U_{23}klb^*c^*)\}$. Atomic coordinates of the hydrogen atoms are given in [10].

Atom	x	y	z	$U_{eq} \times 10^{-1}$/pm^2
Cd(1)	0.2537(1)	0.2500	0.40630(8)	72.6(4)
I(1)	0.04754(8)	0.2500	0.3960(1)	100.2(5)
I(2)	0.3222(1)	0.2500	0.55993(7)	123.5(5)
I(3)	0.32517(7)	0.0167(1)	0.33241(6)	130.2(4)
N(1)	0.150(1)	0.2500	0.101(1)	92(4)
C(11)	0.255(2)	0.2500	0.087(3)	340(20)
C(12)	0.100(3)	0.2500	0.026(20)	340(20)
C(13)	0.111(2)	0.365(3)	0.140(2)	350(20)
N(2)	0.472(1)	0.2500	0.838(1)	72(4)
C(21)	0.437(2)	0.2500	0.757(1)	190(10)
C(22)	0.397(2)	0.2500	0.899(2)	230(20)
C(23)	0.539(2)	0.358(2)	0.858(1)	280(10)

40 ml min^{-1}. The structure was determined using a four circle X-ray diffractometer Stoe IPDS. From the measured intensities, corrected for Lorentz-polarization and absorption effects, the structures were obtained by Fourier synthesis, and refined by least-squares methods with the programs given in [9].

Table 3. Bond distances (pm) and angles (°).

Connection		*d*/pm	Connection		Angle/°
Cd(1)-I(1)		277.3(2)	I(1)-Cd(1)-I(2)		113.08(7)
Cd(1)-I(2)		276.4(2)	I(1)-Cd(1)-I(3)	×2	108.51(4)
Cd(1)-I(3)	×2	277.0(1)	I(2)-Cd(1)-I(3)	×2	108.12(4)
			I(3)-Cd(1)-I(3)$^{\#1}$		110.50(6)
N(1)-C(11)		142(1)	C(11)-N(1)-C(12)		108(3)
N(1)-C(12)		143(1)	C(11)-N(1)-C(13)	×2	116(2)
N(1)-C(13)	×2	140.2(9)	C(12)-N(1)-C(13)	×2	104(2)
N(2)-C(21)		144.2(9)	C(13)-N(1)-C(13)$^{\#1}$		106(3)
N(2)-C(22)		143.5(9)	C(21)-N(2)-C(22)		118(2)
N(2)-C(23)	×2	142.7(9)	C(21)-N(2)-C(23)	×2	116(1)
			C(22)-N(2)-C(23)	×2	105(2)
			C(23)-N(2)-C(23)$^{\#1}$		95(3)

Symmetry Code $^{\#1}$: $x, -y + \frac{1}{2}, z$.

Results and Discussions

The crystal structure of $[N(CH_3)_4]_2CdI_4$ has been reported by Kallel et al. [1]. Our result at 293 K is almost the same as theirs. $[N(CH_3)_4]_2CdI_4$ crystallizes at 293 K orthorhombic Pnma; the experimental conditions and the lattice constants etc. are listed in Table 1. Table 2 lists the positional coordinates and equivalent thermal parameters U_{eq} [10]. Bond distances and angles are listed in Table 3. The average Cd-I bond distance is 276.9(4) pm, the average C-N distance 142(2) pm. Figure 1 shows the projection of the unit cell along [010] onto the *ac* plane. The thermal displacement parameters of the cations and anions are large. This is usually observed in a Pnma phase of $[N(CH_3)_4]_2MX_4$ (M = Zn, Cd, Hg; X = Cl, Br, I) and is successfully explained by an order-disorder model or a split atom one [3 - 6, 8]. The observed C-N bond distances in $[N(CH_3)_4]_2CdI_4$ are a little shorter than usual, which is well understood if C atoms have two close disordered sites. In ^{1}H NMR spin-lattice relaxation measurements of $[N(CH_3)_4]_2CdI_4$, Sato et al. found a cationic thermal motion with a very low activation energy that can be attributed to a small-angle reorientation of cations between two orientations [2]. Moreover, the observed value of the transition entropy also supports a disordering of anions and cations in $[N(CH_3)_4]_2CdI_4$, as shown below.

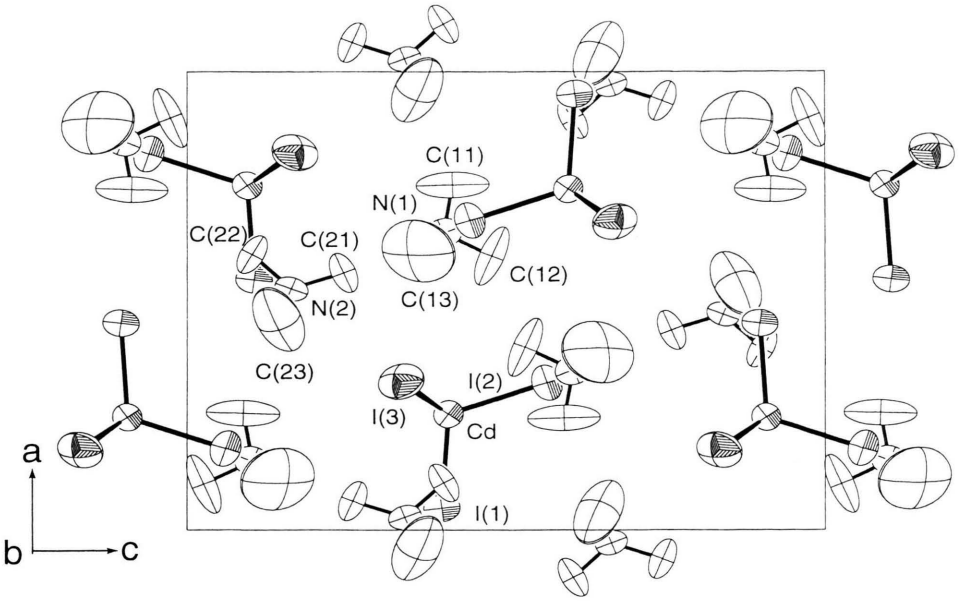

Fig. 1. Projection of the unit cell along [010] onto the *ac* plane.

The DSC measurement was done from 130 K up to 570 K. Above ca. 630 K, the compound melted with decomposition. The first-order phase transition occurs at 245 K (the temperature hysteresis = 1 K, transition enthalpy ΔH = 1.3 kJ mol^{-1}, transition entropy ΔS = 5.4 J K^{-1} mol^{-1}). This phase transition is considered to be of an order-disorder type. On the other hand, Sato et al. reported that two successive phase transitions exist around 244 K, based on the observed DTA curve having a shoulder [2]. We did not observe a shoulder on a DSC peak. $[N(CH_3)_4]_2MBr_4$ (M = Zn, Cd, Hg) and $[N(CH_3)_4]_2HgCl_4$ undergo a single second-order phase transition ($P2_1/c \leftrightarrow Pmcn$) around room temperature [4 - 7, 11 - 13]. $[N(CH_3)_4]_2ZnI_4$ has two phase transitions, one is of second order (255 K, $P2_1/c \leftrightarrow Pmcn$), and the other of first-order (218 K, $Pbc2_1 \leftrightarrow P2_1/c$) [8, 14]. $[N(CH_3)_4]_2HgI_4$, which showed an NQR temperature dependence very similar to $[N(CH_3)_4]_2CdI_4$, has a single first-order phase transition at 272 K [12]. $[N(CH_3)_4]_2CdI_4$ has another first-order phase transition at 527 K (ΔH = 0.2 kJ mol^{-1}, ΔS = 0.4 J K^{-1} mol^{-1}). This transition might be of a displacive type because of its small transition entropy. The phase above 527 K is stable on cooling down to room temperature.

The dependence of the transition points from the low-temperature to the Pnma phase in $[N(CH_3)_4]_2MX_4$ (M = Zn, Cd, Hg; X = Cl, Br, I) on the unit cell volume of the Pnma phase is shown in Figure 2.

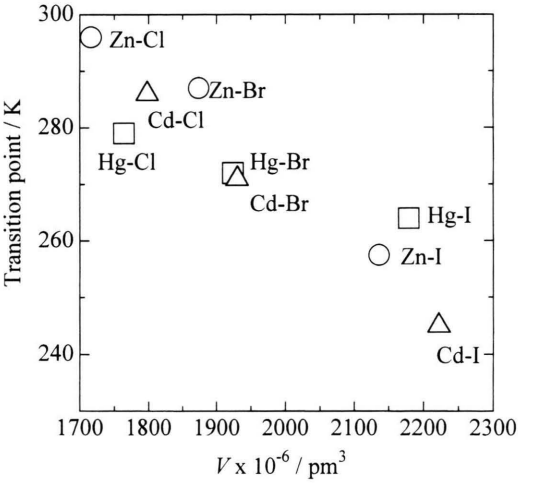

Fig. 2. The dependence of the transition points from the low-temperature to the Pnma phase on the unit cell volume (V) of the Pnma phase. The compounds $[N(CH_3)_4]_2MX_4$ (M = Zn, Cd, Hg, X = Cl, Br, I) are abbreviated as M-X. The data of transition points refer to: Zn-Cl [15], Zn-Br [13, 16], Zn-I [14], Cd-Cl [2], Cd-Br [2, 6, 11], Cd-I [2, this work], Hg-Cl [12, 17], Hg-Br [12], Hg-I [12]; the data of volumes refer to: Zn-Cl [3] , Zn-Br [5, 18], Zn-I [8], Cd-Cl [2], Cd-Br [6], Cd-I [1, this work], Hg-Cl [4, 7], Hg-Br [7], Hg-I [7].

The transition points decrease with the increasing size of the unit cell. This volume dependence in the Hg group is weaker than in the Zn and Cd groups. The effect of hydrostatic pressure on the phase transitions

Table 4. ^{127}I NQR frequencies at several temperatures.

Temperature		ν/MHz
Liquid nitrogen temperature	ν_1	79.57, 81.86, 82.56, 83.36, 84.68, 87.72, 88.34, 88.86
Liquid nitrogen temperature	ν_2	156.70, 161.02, 163.40, 165.70, 167.04, 172.77, 173.51, 174.51
252 K	ν_1	81.00(1), 79.81(1), 78.29(2)
293 K	ν_1	80.21(1), 79.50(4), 77.73(2)
296 K	ν_1	80.16(1), 79.44(4), 77.60(2)
293 K	ν_2	158.91

ν_1 and ν_2 are frequencies corresponding to the transitions $m = \pm\frac{1}{2} \leftrightarrow \pm\frac{3}{2}$ and $m = \pm\frac{3}{2} \leftrightarrow \pm\frac{5}{2}$, respectively. The intensity ratios are in parentheses.

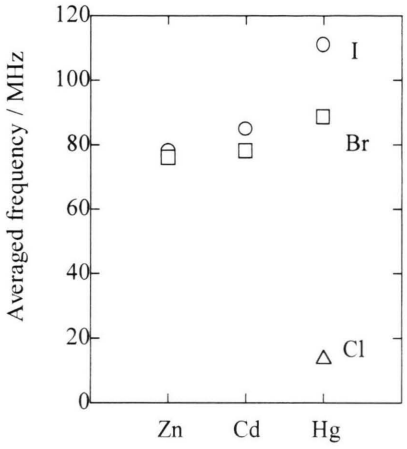

Fig. 3. Comparison of averaged ^{35}Cl, ^{81}Br, and ^{127}I ($m = \pm\frac{1}{2} \leftrightarrow m = \pm\frac{3}{2}$) NQR frequencies in $[N(CH_3)_4]_2MX_4$ (M = Zn, Cd, Hg, X = Cl, Br, I). The NQR frequencies refer to: $[N(CH_3)_4]_2ZnBr_4$ [13], $[N(CH_3)_4]_2ZnI_4$ [14], $[N(CH_3)_4]_2CdBr_4$ [11], $[N(CH_3)_4]_2CdI_4$ [this work], $[N(CH_3)_4]_2HgX_4$ (X = Cl, Br, I) [12].

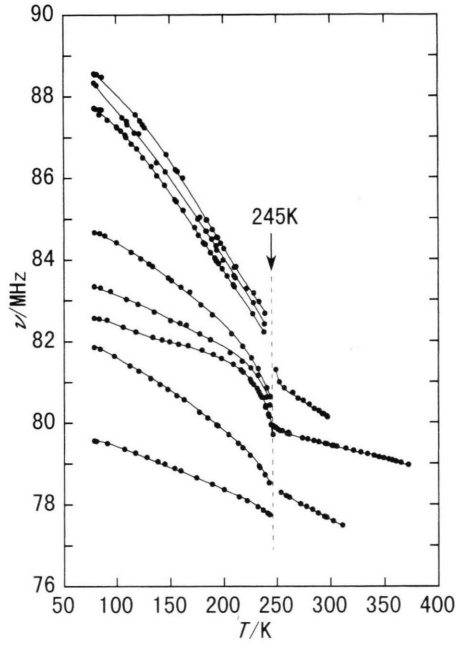

Fig. 4. Temperature dependence of ^{127}I(ν_1) NQR frequencies in $[N(CH_3)_4]_2CdI_4$.

in $[N(CH_3)_4]_2MBr_4$ (M = Zn, Co) has been reported; the temperature of the transition point increases with increasing hydrostatic pressure [19]. These observations suggest that the intermolecular interaction between $[N(CH_3)_4]$ cations and MX_4 anions is a very important factor for the phase transitions in this family.

The ^{127}I NQR frequencies at several temperatures are listed in Table 4. Figure 3 shows averaged NQR frequencies at 77 K of $[N(CH_3)_4]_2MX_4$ (M = Zn, Cd, Hg, X = Cl, Br, I). Since the averaged NQR frequencies increase in the order of Zn, Cd and Hg, the strength or the covalent bond character of M-X bonds seems to increase in the same order. This is expected from the conception of Pearson [20] that soft acids tend to bind to soft bases. The temperature dependence of ^{127}I(ν_1) NQR frequencies is shown in Figure 4. Eight ^{127}I(ν_1) NQR lines and corresponding ^{127}I(ν_2) NQR lines were observed at liquid nitrogen temperature. These lines could be observed up to the transition point at 245 K. Three NQR lines with an intensity ratio of 1:1:2 in the order of decreasing frequency were observed just above the transition point. This observation agrees well with the result of the X-ray structure determination. The CdI_4 anion lies on a mirror plane; two iodine atoms in a CdI_4 anion are on the plane, while the other two are on the equivalent sites connected by the mirror plane. Two NQR lines faded out with increasing temperature, as shown in Figure 4. A fade-out like this was also observed in $[N(CH_3)_4]_2HgI_4$ [12] and $[N(CH_3)_4]_2ZnI_4$ [14]. This phenomenon is probably explained as follows. Since an MX_4 tetrahedron has four pseudo C_3 symmetry

axes that run through each X atom, four kinds of C_3 rotations can be thermally excited. Since there are three kinds of iodine atoms in a CdI_4 tetrahedron, the C_3 rotations can fluctuate the electric field gradients at iodine nuclei and make relaxation times short enough to broaden the line widths beyond the limits of observation. If a single C_3 rotation is excited more strongly than the other three, only a resonance line due to an iodine atom lying in the C_3 axis, around which a thermal motion is excited, is observable and the other two lines may disappear.

The overall temperature behavior of NQR frequencies in the title compound is very similar to that of $[N(CH_3)_4]_2HgI_4$ [12] but different from those of $[N(CH_3)_4]_2MBr_4$ (M = Zn, Cd, Hg) and $[N(CH_3)_4]_2HgCl_4$ [11, 12, 13]. Especially the number of NQR lines in the low-temperature phase is different, i.e. $[N(CH_3)_4]_2MBr_4$ (M = Zn, Cd, Hg) and $[N(CH_3)_4]_2HgCl_4$ have four Br or Cl NQR lines, but $[N(CH_3)_4]_2CdI_4$ and $[N(CH_3)_4]_2HgI_4$ have eight ^{127}I NQR lines. The temperature dependences of ^{127}I NQR frequencies in the low-temperature phase below 218 K and the high-temperature phase above 255 K of $[N(CH_3)_4]_2ZnI_4$ are very similar to those in each corresponding phase of $[N(CH_3)_4]_2CdI_4$ and $[N(CH_3)_4]_2HgI_4$. The phase below 218 K of $[N(CH_3)_4]_2ZnI_4$ has a structure of $Pbc2_1$ and eight ^{127}I NQR lines. Sato et al. suggested that more than two nonequivalent cations exist in the low-temperature phase of $[N(CH_3)_4]_2CdI_4$ from the measurement of ^{1}H NMR [2]. Accordingly the structure of the low-temperature phase of $[N(CH_3)_4]_2CdI_4$ seems to be similar to or the same as $Pbc2_1$.

[1] A. Kallel, J. W. Bats, and A. Doud, Acta Crystallogr. **B37,** 676 (1981).

[2] S. Sato, R. Ikeda, and D. Nakamura, Bull. Chem. Soc. Japan **59,** 1981 (1986).

[3] K. Hasebe, H. Mashiyama, N, Koshiji, and S. Tanisaki, J. Phys. Soc. Japan **56,** 3543 (1987).

[4] T. Asahi, K. Hasebe, and K. Gesi, J. Phys. Soc. Japan **60,** 921 (1991).

[5] T. Asahi, K. Hasebe, and K. Gesi, J. Phys. Soc. Japan **57,** 4219 (1988).

[6] T. Asahi, K. Hasebe, and K. Gesi, J. Phys. Soc. Japan **61,** 1590 (1992).

[7] B. Kamenar and A. Nagal, Acta Crystallogr. **B32,** 1414 (1976).

[8] M. L. Werk, G. Chapius, and F. J. Zuniga, Acta Crystallogr. **B46,** 187 (1990).

[9] G. M. Sheldrick, SHELX86, Program for the solution of crystal structures, University of Gottingen, Germany 1990. SHELX 93, Program for crystal structure determination. University of Gottingen, Germany 1993.

[10] Tables of the atomic coordinates including hydrogen atoms, thermal parameters, bond distances and angles have been deposited as CCDC 133335 at the Cambridge Crystallographic Data Center.

[11] H. Ishihara, K. Horiuchi, Shi-qi Dou, T. M. Gesing, J. C. Buhl, H. Paulus, and H. Fuess, Z. Naturforsch. **53a,** 717 (1998)

[12] H. Tearo, T. Okuda, K. Yamada, H. Ishihara, and Al. Weiss, Z. Naturforsch. **51a,** 755 (1996).

[13] R. Perret, Y. Beaucamps, G. Godefroy, P. Muralt, M. Ehrensperger, H. Arend, and D. Altermatt, J. Phys. Soc. Japan **52,** 2523 (1983); H. Tada, H. Nakayama, and N. Nakamura, Z. Naurforsch. **53a,** 459 (1998).

[14] J. Pirnat, J. Lužnik, Z. Trontelj, and P. K. Kadaba, Z. Naturforsch. **45a,** 349 (1990).

[15] S. Sawada, Y. Shiroishi, A. Yamamoto, M. Takashige, and M. Matsuo, J. Phys. Soc. Japan **43,** 2099, 2101 (1977); S. Tanisaki, and H. Mashiyama, J. Phys. Soc. Japan **48,** 33 (1980).

[16] K. Gesi, J. Phys. Soc. Japan **51,** 203 (1982).

[17] K. Gesi, Phase Transitions **27,** 107 (1990).

[18] P. Trouelan, J. Lefebvre, and P. Derollez, Acta Crystallogr. **C40,** 386 (1984).

[19] K. Gesi and K. Ozawa, J. Phys. Soc. Japan **52,** 2440 (1983).

[20] R. G. Pearson, "Survey of Progress in Chemistry, 1", A. Scott ed., Academic Press, New York 1969, Chapt. 1.